TECHNICAL REPORT

Algorithm for Automatic Detection, Localization and Characterization of Magnetic Dipole Targets Using the Laser Scalar Gradiometer

ESTCP Project MR-201612

JUNE 2016

Leon Vaizer
Jesse Angle
Neil Claussen
Naval Surface Warfare Center,
Panama City Division

ESTCP

REPORT DOCUMENTATION PAGE

Form Approved
OMB No. 0704-0188

1. REPORT DATE *(DD-MM-YYYY)*	2. REPORT TYPE	3. DATES COVERED *(From - To)*
07/05/2016	Techncial Report	March - June, 2016

4. TITLE AND SUBTITLE
Algorithm for Automatic Detection, Localization and Characterization of Magnetic Dipole Targets Using the Laser Scalar Gradiometer

5a. CONTRACT NUMBER

5b. GRANT NUMBER

5c. PROGRAM ELEMENT NUMBER

6. AUTHOR(S)
Leon Vaizer, Jesse Angle, Neil Claussen
Naval Surface Warfare Center, Panama City Division

5d. PROJECT NUMBER
MR-201612

5e. TASK NUMBER

5f. WORK UNIT NUMBER

7. PERFORMING ORGANIZATION NAME(S) AND ADDRESS(ES)
Naval Surface Warfare Center, Panama City Division
110 Vernon Ave
Panama City, FL 32407

8. PERFORMING ORGANIZATION REPORT NUMBER

9. SPONSORING/MONITORING AGENCY NAME(S) AND ADDRESS(ES)
Environmental Security Technology Certification Program (ESTCP)
4800 Mark Center Drive
Suite 17D08
Alexandria VA 22350-3600

10. SPONSOR/MONITOR'S ACRONYM(S)
ESTCP

11. SPONSOR/MONITOR'S REPORT NUMBER(S)

12. DISTRIBUTION/AVAILABILITY STATEMENT
Approved for public release; distribution is unlimited.

13. SUPPLEMENTARY NOTES
N/A

14. ABSTRACT
The objective of this project will be to create a software toolbox available from within Geosoft's Oasis montaj geophysical analysis software package, similar to the land based UXO detection tools developed by the Army. A selection of algorithms and software tools developed at the Naval Surface Warfare Center will be properly packaged and combined with appropriate tools already available within Oasis montaj to allow for magnetic gradiometric data collected from these systems to be analyzed and displayed in a manner similar to other electromagnetic unexploded ordnance detection systems currently in use by the DoD.

15. SUBJECT TERMS
N/A

16. SECURITY CLASSIFICATION OF:			17. LIMITATION OF ABSTRACT	18. NUMBER OF PAGES	19a. NAME OF RESPONSIBLE PERSON
a. REPORT	b. ABSTRACT	c. THIS PAGE			Dr. Jesse Angle
U	U	U	UU	11	19b. TELEPHONE NUMBER *(Include area code)*: 850-636-6458

TABLE OF CONTENTS

LIST OF ACRONYMS

AUV – Autonomous Underwater Vehicle
CN – Confidence Number
EOD – Explosive Ordnance Disposal
INS – Inertial Navigation System
LLS – Linear Least Squares
LSG – Laser Scalar Gradiometer
NSWCPCD – Naval Surface Warfare Center, Panama City Division
ONR – Office of Naval Research
rms – root-mean-square

LIST OF FIGURES

INTRODUCTION

This paper describes an automatic algorithm that detects, localizes and characterizes magnetic targets from the measurements collected by the Laser Scalar Gradiometer (LSG) residing onboard an Autonomous Underwater Vehicle (AUV). Magnetic sensors such as the LSG provide information that is independent of acoustic measurements and can thus be used to improve target classification. The LSG, developed by Polatomic Inc. for mine countermeasures using funding from the Office of Naval Research (ONR) and Navy Explosive Ordnance Disposal (EOD) and shown in **Figure 1**, features four high sensitivity laser pumped Helium cells that measure the magnitude of the local magnetic field at four separate points by measuring changes in the Larmor precession frequency. These cells are arranged in such a way as to allow three nearly orthogonal scalar-field differences (gradients). Using field differences cancels the effects of distant sources of magnetic noise and helps with target resolution. The described algorithm operates on overlapping segments of data which are compensated for platform motion noise. The algorithm attempts to fit each segment of measured data with a minimal number of magnetic dipoles by iteratively adding dipoles, optimizing their positions and removing unnecessary dipoles. The algorithm requires no operator involvement in the target localization process and has been modified to run in real time, onboard the AUV, with a short delay necessary to accumulate sufficiently long segment of data.

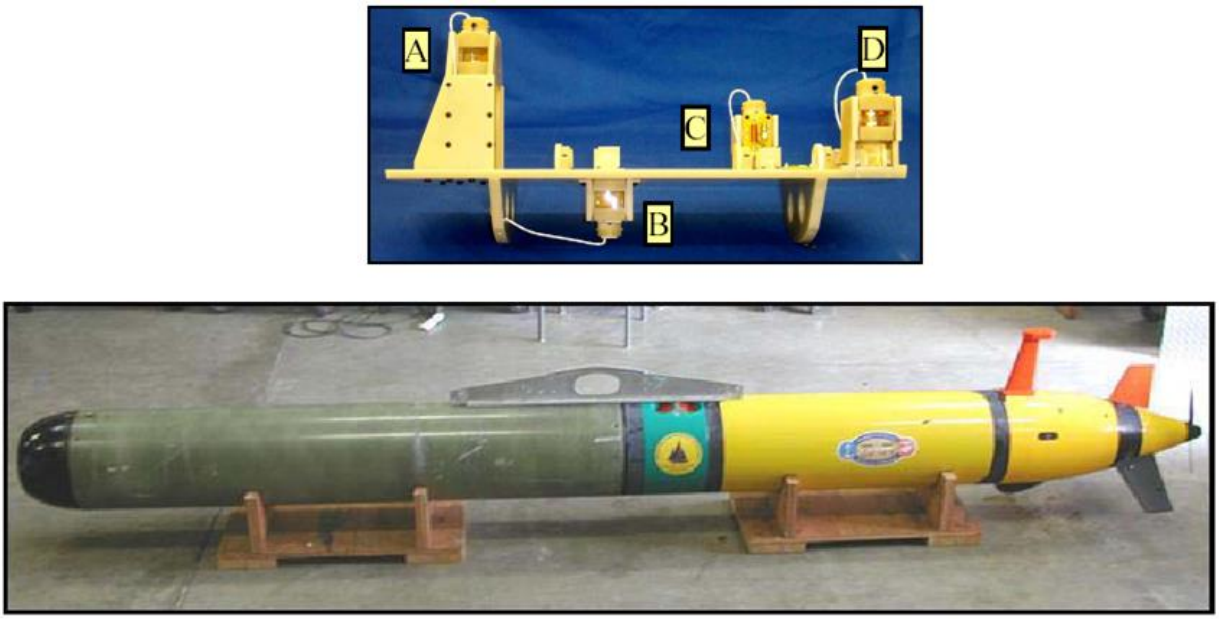

Figure 1: LSG cell assembly (top) and REMUS600 AUV with LSG sensor payload located in the forward section (bottom).

SIGNAL MODEL

LSG collects a time history of the magnetic field magnitude at its four cells as it passes through the field. A magnetic source will appear point-like if the sensor is not too close to the source (farther than once or twice than the dimensions of the target) and can be approximated as a dipole. The sensor's position and orientation are provided by the AUV's Inertial Navigation System (INS). The incoming magnetic signal is conditioned, low-pass filtered down to the

frequency band of interest (usually 1 Hz and below) and down-sampled. Navigation data comes in at a different rate and is low pass filtered to the same frequency band as the magnetic data and then interpolated to the exact time of down-sampled magnetic signal. Because both magnetic and navigation data streams are buffered and delayed for processing times, a relative delay between data streams is calculated to align data as closely as possible, typically only following hardware modifications and not as a standard operating procedure. The coordinate system that is used is North, East, and Down.

Each cell measures the sum of background field and field due to the dipole. Since Earth's magnetic field is much bigger than the target field, the signal at the cell may be approximated as

$$C = \left|\vec{E} + \vec{B}\right| \approx \left|\vec{E}\right| + \vec{e} \cdot \vec{B} = \left|\vec{E}\right| + \vec{e} \cdot \left(\frac{\mu_0}{4\pi}\left(\frac{3\vec{r}(\vec{m} \cdot \vec{r})}{r^5} - \frac{\vec{m}}{r^3}\right)\right)$$

where

$\vec{E}$ and $\vec{e}$ are Earth's magnetic field and its respective unit vector
$\vec{B}$ is the target's magnetic field
$\vec{m}$ is the dipole magnetic moment of the target
$\vec{r}$ is the vector distance from dipole to sensor
μ_0 is the permeability constant for free space

Differencing cell signals removes background field that consists of Earth's field and any time-varying geodesic noise as well as common electronic noise generated by the host platform.

ALGORITHM APPROACH

The algorithm for processing LSG data closely follows the algorithm developed at NSWCPCD in the 1990's for superconducting gradiometers [1]. The signals used for analysis consist of three cell differences along predominantly cardinal directions in the platform body frame as well as the signal at the most forward cell. The forward cell is chosen because it is farthest from platform noise sources which are typically located at the rear of the vehicle. It is still subject to much more noise than the differences and is significantly de-weighted relative to cell differences.

At any instant in time we have field measurements at four cells whose positions in global coordinate system are known. The difference signal between cells *i* and *j* due to dipole *T* is given by

$$S_{ij}(t) = \vec{e} \cdot \frac{\mu_0}{4\pi}\left[\left(\frac{3\vec{r_i}(t)\left(\vec{m} \cdot \vec{r_i}(t)\right)}{{r_i}^5(t)} - \frac{\vec{m}}{{r_i}^3(t)}\right) - \left(\frac{3\vec{r_j}(t)\left(\vec{m} \cdot \vec{r_j}(t)\right)}{{r_j}^5(t)} - \frac{\vec{m}}{{r_j}^3(t)}\right)\right] + \eta_{ij}(t)$$

where

$\vec{r_i}$ and $\vec{r_j}$ are distance vectors from the dipole to cells *i* and *j*
η(t) is a noise term due to platform motion, magnetic noise generated by platform subsystems and total field gradient due to more distant ferrous objects

We make an attempt to compensate $S_{ij}(t)$ for $\eta_{ij}(t)$. *S(t)* is linear with respect to dipole magnetic moment $\vec{m} = (m_N, m_E, m_d)$ so $\vec{m}$ can be calculated if the number of dipoles comprising *S(t)* and their positions are known.

To estimate a dipole's position we first perform grid search at a few locations on the bottom. The location that best fits the observed signal is chosen as an initial pick. Standard iterative gradient search is used to refine the position.

$$\left(\hat{m} : \widehat{\Delta x}\right) = \left(\left[\frac{\partial \vec{S}}{\partial \vec{m}}\right]_{\vec{p}=\hat{p}} : \left[\frac{\partial \vec{S}}{\partial \vec{p}}\right]_{\vec{m}=\hat{m},\vec{p}=\hat{p}}\right)^{-1} \left[\vec{S}\right]^T$$

where

$\hat{m}$ is the estimated dipole moment
$\hat{p}$ is the estimated dipole position
$\widehat{\Delta x}$ is a correction to the dipole position
$\vec{S}$ consists of 3 total field differences and 1 total field signal for all points in the window

All partial derivatives are calculated analytically. If the fit to the measured signal is not satisfactory, the process is repeated by searching the grid for best starting position of another dipole and optimizing positions of all dipoles. After each dipole addition cycle, each dipole is evaluated and assigned a Confidence Number (CN). CN is a function of signal fit, measure of how effectively each dipole reduces signal residuals and some heuristic factors (e.g. proximity to other dipoles, how close the dipole's estimated location is to the segment window center, reasonableness of the estimated dipole magnitude and estimated position). The dipoles are ranked by CN, and if the number of dipoles exceeds preset limits, the dipole with the lowest CN is removed and positions of the remaining dipoles are optimized. The process repeats until the signal fit is satisfied or the number of iterations exceeds the predetermined limit. Logic was added to prevent the algorithm from looping where the same dipole is repeatedly added and then removed.

If one dipole is present, convergence to the dipole's true position is usually quick. In a small number of cases where the algorithm converges to a local residual minimum, adding another dipole reshapes the residual space, allowing one of the dipoles to reach a global minimum after which the extra dipole is removed. In the case of multiple dipoles, the single segment solution is accurate if the magnetic field peaks due to the dipoles are sufficiently separated. If there is a significant overlap in the signals due to multiple dipoles, for instance when the dipole separation is less than the long axis of the targets, thus causing the far field signal to blur into an approximate single target, sometimes the dipoles are not easily separable. For a superconducting gradiometer, where five gradients are typically available, the multiple dipole problem was much more observable, but with LSG, with only three total field differences, we have less information available, and the multiple dipoles may not be observable in some situations. An example would be the sensor passing in a straight line between two equal dipoles. A way to resolve the dipoles in this situation is to use more than one track at a time.

NOISE MITIGATION

Major magnetic noise sources are due to platform subsystems, effects of platform's permanent and induced field as it rotates within Earth's field and total field gradients due to more distant ferrous objects. While appropriate mission planning and vehicle operation can limit the amount of noise generated, appropriate signal processing steps are taken to maximize usability of data.

Platform Subsystems-Generated Noises

The AUV platform is constructed of mostly non-ferrous materials. Still, it is an electrically-powered AUV with actuators, propulsors, batteries and current-carrying cables. Other co-residing sensors such as sidescan sonar and electro-optic camera as well as communication systems also generate electromagnetic noise. Modeling all of these noise sources is difficult. To alleviate the noise burden the magnetic sensor was placed as far forward as possible away from these noise sources and the magnetic signal is filtered down to a minimal bandwidth of interest. Whenever the system reports that an intermittent activity is taking place that is likely to generate magnetic noise (such as communication ping or very high controller activity in parts of turns) the magnetic signal is de-weighted to minimize corrupting effects from such an activity.

Motion Noise

A version of the Tolles-Lawson noise reduction model has been developed to apply to multi-channel gradiometers. The model was developed for airborne systems and uses auxiliary fluxgate measurements to estimate signal due to platform permanent and induced moments rotating in Earth's field [2]. Because our fluxgate is located much closer to noise-generating subsystems than the LSG sensors, and to avoid added complexity of removing the effects of near targets from fluxgate measurements, we synthesize fluxgate measurements from nominal value of background field and INS measurements. Tolles-Lawson coefficients that are used to compensate the signal for motion-generated noise are calculated from specially designed maneuvers that minimize non-motion dependent noise, and, if collected target data is clean enough, from mission data itself. Unlike airborne systems for which the Tolles-Lawson model was developed, the underwater systems can exercise a much more limited range of motions. As a result, some Tolles-Lawson coefficients may be linearly dependent. To address this issue, a maximum non-singular subset of coefficients is estimated adaptively and all sections of data with significant contributions from non-motion related sources of the magnetic signal (i.e. signal due to platform control activity, activity of co-located sensors or clutter of no interest) are identified and de-weighted when computing motion coefficients. Each cell difference is processed independently.

Background Gradient

Significant field gradients due to large sources separate from the target of interest cannot always be captured completely by the length of the data window. In order to locate targets in such an environment, it is important to reduce this background as much as possible. We model the background gradient by a polynomial that is included in our list of parameters estimated using Linear Least Squares (LLS) together with dipole parameters and use this to further enhance the signal.

COMBINING MULTIPLE RUNS

Window Size

Ideally, we would like the signal due to a dipole to take up half of our signal window and be centered within that window. When we operate in an environment where dipole size and density are unknown, we run the algorithm repeatedly each time using window size optimized for different size targets. The windows overlap by 50% and we want to make sure that all targets of interest are in the middle half of one of the windows.

Number of Dipoles

Because the target density is unknown, we run the algorithm for a different number of targets per segment. We use the CN assigned to each localization to sort between different looks at the same target. Picking the localization with the highest CN usually gives us the most accurate estimate of the target magnetic moment.

EXAMPLES

In **Figure 2** we show the effects of motion compensation. The uncompensated signal may be usable for bigger targets of interest, but clearly motion compensation is crucial to get accurate signal due to smaller targets that might otherwise be missed. The data shown contains five targets, at sample numbers 295, 465, 1100, 1190 and 1300. The particular target of interest is at sample 295 and is swamped by motion noise in (a), can be seen in (b) after compensation with pre-computed Tolles-Lawson coefficients, and is cleaned up farther in (c) after correcting motion coefficients. Residual signal root-mean-square (rms) is reduced 18 dB from (a) to (b), and 22 dB from (a) to (c).

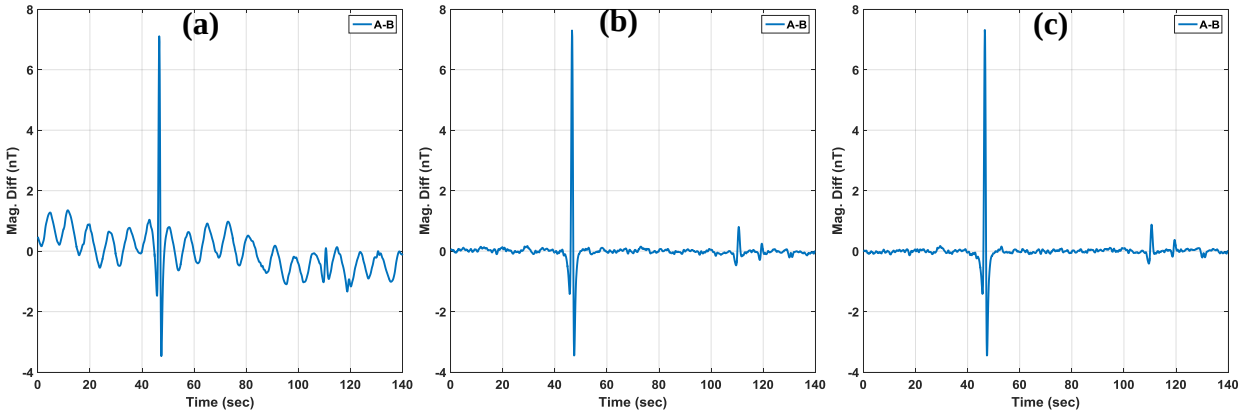

Figure 2: Example of signal improvement due to Motion Compensation, showing the uncompensated signal (a), signal compensation using pre-computed Tolles-Lawson coefficients (b) and final signal compensation using corrected coefficients (c).

A fit to the measured signal is shown in **Figure 3**. Estimating target position accurately allows accurate estimate of the target's dipole moment which in turn allows us to calculate whether the target is consistent with an intact ferrous cylinder's induced moment, and under certain assumptions, allows us to estimate that cylinder's orientation and dimensions [3]. The residual

signal shows effects of early termination process and there may be artifacts of residual platform noise as well.

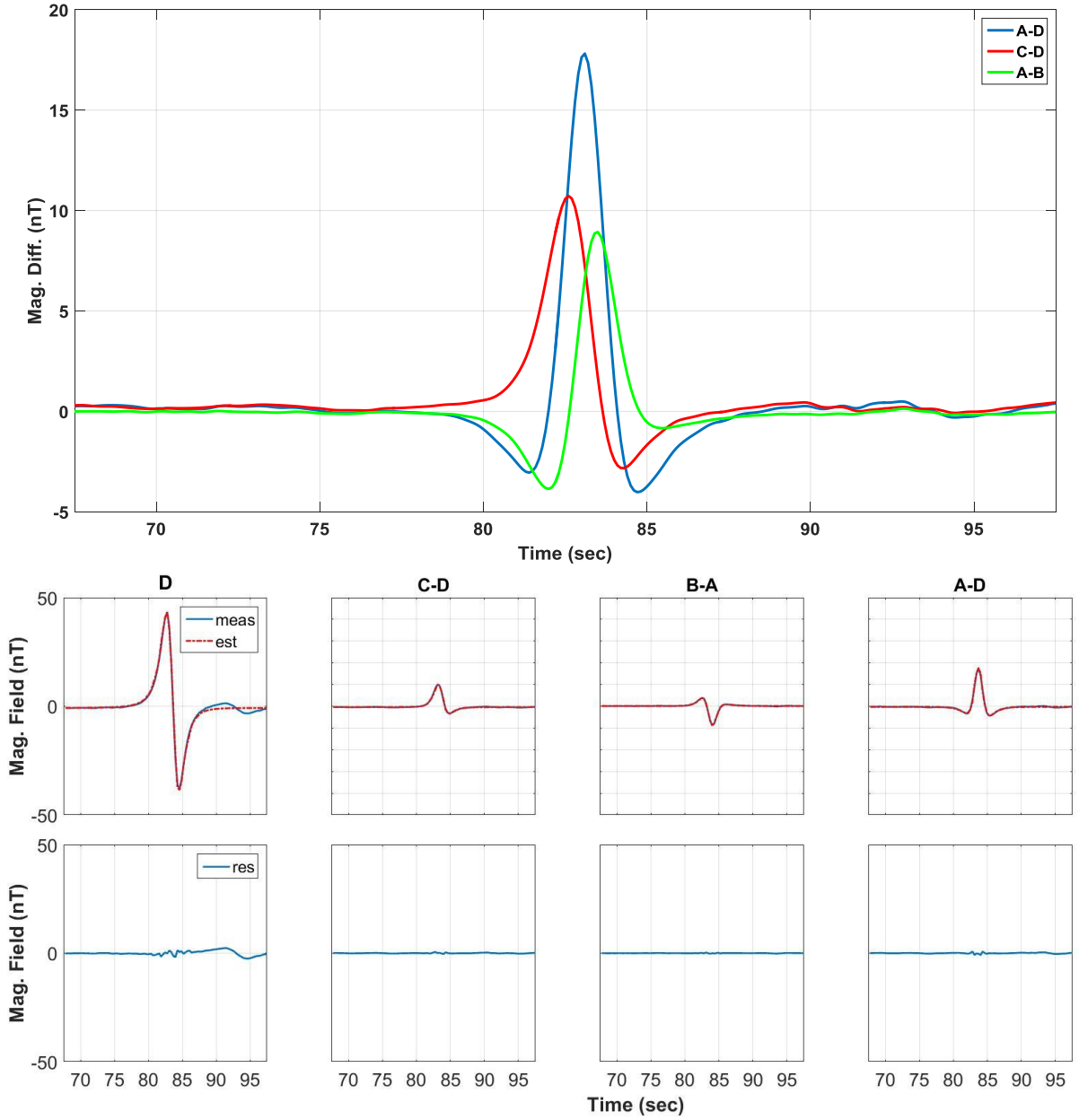

Figure 3: The top plot shows the three measured gradients centered within the data window. The middle row of plots show the individual gradients and a single measurement from the D cell (far left) along with the associated estimated signal due to the target dipole. The bottom row of plots show the residual signal remaining after subtracting the measured and estimated signals.

A mission consisting of a few passes past a target of interest is shown in **Figure 4**. AUV tracks in the upper left image are displayed in blue (portions of turns were not recorded). Localized targets are shown with red triangles for high confidence localizations and green for medium confidence localizations. The small plot in the upper right zooms on an area around a particular

target of interest. Each pass by the target generated independent localizations. From the zoomed plot all localizations lie essentially on top of each other, well within track-to-track navigation accuracy. The waveforms for both the three differences and the total-field signals are displayed as well on the right. From the waveform we can see a larger target (the one we were investigating) and a smaller target a significant distance away. The table shows the estimated target position relative to the LSG, as vertical and horizontal offsets, as well as estimated target magnetic moment magnitude and vector for each pass. The localizations are shown in two groups – five for the bigger target and two for the smaller. All estimated moments are consistent with each other. The estimated vertical offset for the larger target (or depth of some dipole-equivalent point inside the target's body) relative to the sea floor is close to zero implying it is proud on the surface. Furthermore, the moment is consistent with the induced moment for a horizontal cylinder. The vertical offset of the smaller target relative to the sea floor is estimated to be less than zero, implying that the target is likely to be buried.

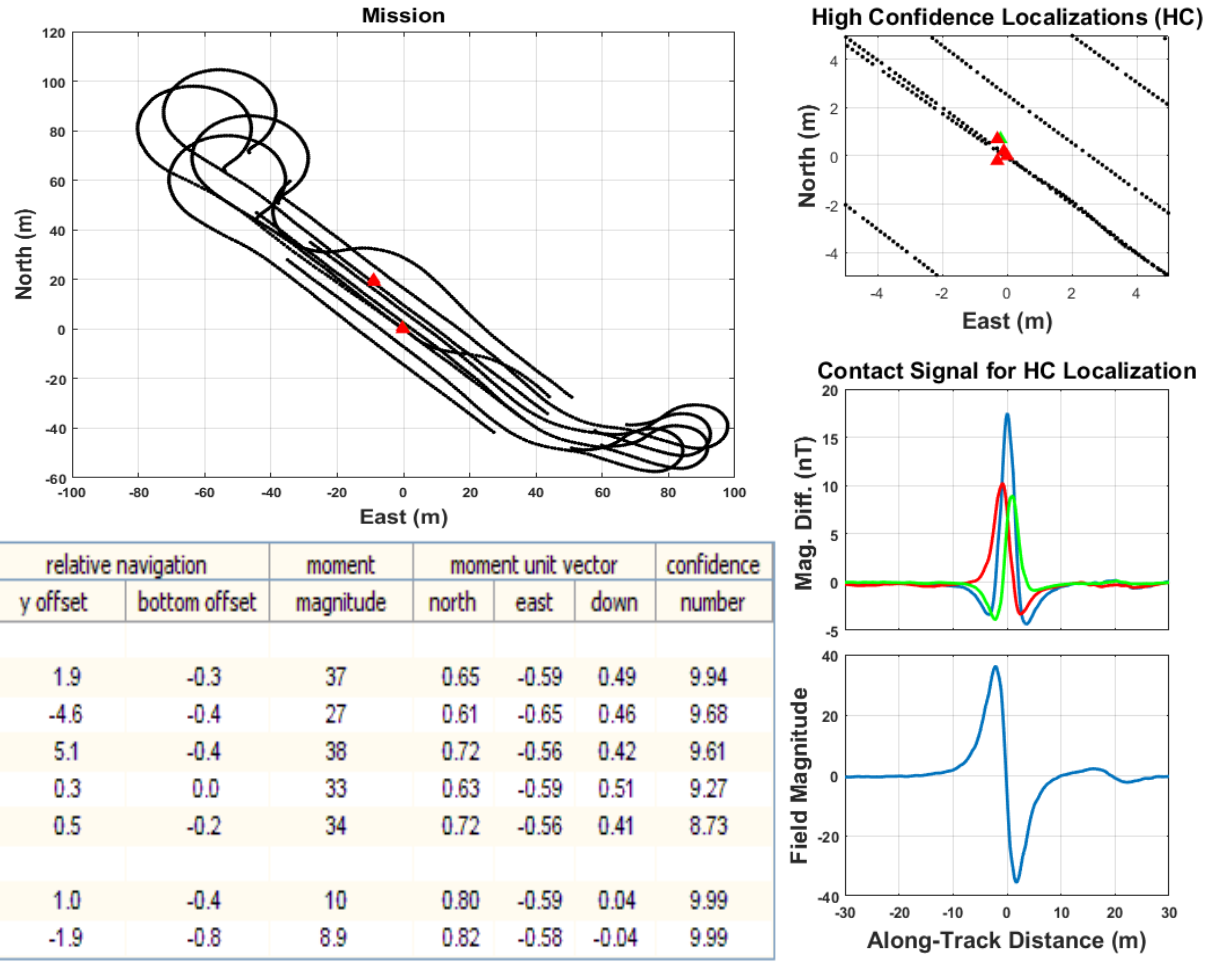

relative navigation		moment	moment unit vector			confidence
y offset	bottom offset	magnitude	north	east	down	number
1.9	-0.3	37	0.65	-0.59	0.49	9.94
-4.6	-0.4	27	0.61	-0.65	0.46	9.68
5.1	-0.4	38	0.72	-0.56	0.42	9.61
0.3	0.0	33	0.63	-0.59	0.51	9.27
0.5	-0.2	34	0.72	-0.56	0.41	8.73
1.0	-0.4	10	0.80	-0.59	0.04	9.99
-1.9	-0.8	8.9	0.82	-0.58	-0.04	9.99

Figure 4: Summary of an LSG mission. The top-left image shows the vehicle tracks over two targets while the upper right image shows a zoomed in plot around one of the targets, displaying the accuracy of multiple localizations. The other plots on the right show the gradients and field magnitude of a particular track over these targets. The table on the left contains typical target information for the multiple localizations of these two items.

CONCLUSION

The LSG localization algorithm, developed to find ferrous objects of interest on the seabed (e.g. ferrous case mine shapes), has been described herein. Over the last decade, this algorithm has been extensively tested over many targets and in many different environments and although the algorithm was developed for the LSG system most recently, the principles defined here can be applied to other similar underwater magnetic sensor systems as well. The target position and moment estimates have been consistent for multiple runs against the same targets and have been consistent with other sensor outputs as well as ground truth data when available. This style of sensor and this algorithm set have proven very useful in detecting, localizing and classifying objects of interest, ranging from mine shapes to artillery shells, and continues to be employed in many different scenarios.

REFERENCES

1. L. Vaizer, J. Lathrop, and J. Bono, *"Localization of Magnetic Dipole Targets,"* in *Proceedings of MTS/IEEE OCEANS 2004*, November 2004.
2. S.H. Bickel, *"Small Signal Compensation of Magnetic Fields Resulting from Aircraft Maneuvers"*, in *IEEE Transactions on Aerospace and Electronic Systems*, Vol. AES-15, No. 4, July 1979.
3. J. D. Lathrop, H. Shih, W.M. Wynn, *"Enhanced Clutter Rejection with Two-Parameter Magnetic Classification for UXO (U),"* in *Proceedings of SPIE 1999* Vol. 3710, April 1999